HHS Public Access

Author manuscript

Connect Tissue Res. Author manuscript; available in PMC 2024 January 01.

Published in final edited form as:

Connect Tissue Res. 2023 January ; 64(1): 93–104. doi:10.1080/03008207.2022.2102491.

The Adaptive Response of the Mandibular Condyle to Increased Load is Disrupted by ADAMTS5 Deficiency

Sarah C. Porto[1], **Alexandra Rogers-DeCotes**[2], **Emmaline Schafer**[2], **Christine B. Kern**[2,*]

[1]Department of Health and Human Performance, College of Charleston, Charleston, SC 29424

[2]Department of Regenerative Medicine and Cell Biology, Medical University of South Carolina Charleston, SC 29525

Abstract

Objective: To determine the impact of increased load on the temporomandibular joint (TMJ) from mice deficient in the extracellular matrix protease ADAMTS5.

Materials and Methods: Wire springs exerting 0.5 newtons (N) for 1 hour/day for 5 days (*Adamts5*$^{+/+}$-n=18; - *Adamts5*$^{-/-}$ n=19) or 0.8N for 1 hour/day for 10 days (*Adamts5*$^{+/+}$-n=18; *Adamts5*$^{-/-}$ n=17) were used to increase murine TMJ load. Safranin O-staining was used to determine mandibular condylar cartilage (MCC) morphology. Chondrogenic factors Sox9 and aggrecan were immunolocalized. Microcomputed topography was employed to evaluate mineralized tissues and Tartrate-Resistant Acid Phosphatase staining was used to quantify osteoclasts.

Results: Increased load on the mandibular condyle of *Adamts5*$^{-/-}$ mice resulted in an increase in the hypertrophic zone of mandibular condylar cartilage (MCC) compared to normal load (NL) (P<.01). In the trabecular bone of the mandibular condyle, the total volume (TV), bone volume (BV), trabecular thickness (TbTh) and trabecular separation (TbSp) of the mandibular condyles in *Adamts5*$^{-/-}$ mice (n=27) did not change significantly with increased load, compared to *Adamts5*$^{+/+}$ (n=38) that exhibited significant responses (TV-P<.05; BV-P<.001; TbTh-P<0.01; TbSp-P<0.01). The bone volume fraction (BV/TV) was significantly reduced in response to increased load in both *Adamts5*$^{-/-}$ (P<0.05) and *Adamts5*$^{+/+}$ mandibular condyles (P<.001) compared to NL. Increased load in *Adamts5*$^{-/-}$ mandibular condyles also resulted in a dramatic increase in osteoclasts compared to *Adamts5*$^{-/-}$ NL (P<.001) and to *Adamts5*$^{+/+}$ with increased load (P<01).

Conclusion: The trabeculated bone of the *Adamts5*$^{-/-}$ mandibular condyle was significantly less responsive to increased load compared to *Adamts5*$^{+/+}$. ADAMTS5 may be required for mechanotransduction in the trabeculated bone of the mandibular condyle.

Keywords

Cell differentiation; Cell-matrix interactions; Temporomandibular joint (TMJ); Matrix biology; Matrix metalloproteinases; Extracellular matrix; ADAMTS5; mandibular condyle

*Corresponding author: kernc@musc.edu.

Declaration of Interests: The authors do not have any competing interests to declare.

INTRODUCTION

The load-bearing temporomandibular joint (TMJ) facilitates all mandibular movements, and is comprised of the mandibular condyle, the articulating disc and the fossa eminence of the temporal bone. Temporomandibular joint osteoarthritis (TMJOA) affects over 20 million Americans with an annual estimated treatment cost of $4 billion [1–4]. The TMJ is made up of fibrocartilage which is different than hyaline cartilage that is found in the knee and hip. Since most joint studies focus on the knee, the lack of understanding fundamental aspects of fibrocartilage biology [1] is a major obstacle to developing regenerative therapies and treatment of TMJ disorders.

TMJ fibrocartilage is a unique layered structure organized into four zones based on extracellular matrix (ECM) composition and maturational cell type (superficial, polymorphic, chondrocytic and hypertrophic). In the mandibular condylar cartilage (MCC), the upper superficial zone contains stem cells and secretes factors into the synovial space to reduce friction during joint movement. Cells of the polymorphic zone display a fibroblastic and/or mesenchymal phenotype and differentiate into chondrogenic cells. The chondrocytic layer is formed by differentiating chondroblasts that are organized into axial rows with shared cartilage ECM. The adjacent hypertrophic zone contains enlarged cells with a distinct pericellular matrix that contains the cartilage proteoglycan aggrecan (Acan), and a clear intracellular space, giving the classic appearance of hypertrophic chondrocytes; these cells reside in the deepest layer of the MCC, and are adjacent to trabeculated bone. A distinctive characteristic of the mandibular condylar fibrocartilage is that a significant portion of the hypertrophic chondrocytes transdifferentiate into subchondral bone cells [5–7]. Factors involved in the cellular transdifferentiation from hypertrophic chondrocytes to bone forming cells have not been well-described.

The maintenance of healthy TMJ fibrocartilage requires adaptability in response to altered mechanical load. Failure to maintain integrity of the MCC through remodeling leads to TMJ disease. Osteoarthritic disease correlates with upregulated ECM proteases and loss of a proteoglycan-rich matrix [8–10]. Upregulation of the proteoglycanase **A D**isintegrin **A**nd **M**etalloproteinase with **T**hrombo**S**pondin motifs (ADAMTS)-5 and cleavage of its substrate Acan, the most abundant proteoglycan in cartilage, [11, 12] is considered a contributing factor to TMJOA [13–15]. Therefore, reduction of ADAMTS5 activity may protect the TMJ fibrocartilage by promoting Acan stability in the ECM. However, recent studies indicate ADAMTS5 plays an essential physiological role in establishing the zonal organization and identity of cells within each layer of the mandibular condylar fibrocartilage [16] and is critical for normal trabeculated bone development [17]. Mechanisms by which the appropriate balance of proteoglycans and their corresponding proteases are controlled within the TMJ have not been determined.

Since ECM architecture is regulated in response to altered mechanical load, it follows that ECM proteases may serve as components that are critical for mechanotransduction in the TMJ. The objective of this study was to determine if changes in the mandibular condyle due to ADAMTS5 deficiency, result in an altered response to increased load. We anticipate that

these studies will advance our understanding of mechanisms that allow the ECM to adapt to changes in biomechanical forces, fundamental aspects of TMJ biology and regenerative therapies.

Materials and Methods:

Generation of Adamts5$^{-/-}$ Mice:

Animal protocols were approved by the Medical University of South Carolina Institutional Animal Care and Use Committee (IACUC). The standard twelve-hour light cycle was diurnal. There was unlimited access to food and water, supplied via reverse osmosis system and dispensed into Lab Product rodent bottles/sippers. Purina Lab Diet 5V75 (standard diet) and 5VM5 (breeder diet) were utilized with unlimited supply and access. The *Adamts5*$^{-/-}$ mice (*Adamts5*$^{tm1Dgen/J}$, The Jackson Laboratory, Bar Harbor, ME) were bred into C57BL/6J (> 20 generations) and maintained as previously described [18, 19]. Genotyping of *Adamts5* mice was performed using PCR [19]. *Adamts5*$^{-/-}$ mice do not exhibit any pain or distress. Euthanasia protocols for each age endpoint have been approved by IACUC.

TMJ mechanical loading model:

A non-invasive forced open mouth model was used as previously published [20–22] with modifications. Six and a half-week-old male and female C57Bl/6 *Adamts5*$^{+/+}$ or *Adamts5*$^{-/-}$ mice were subjected to forced mouth opening with custom-made β-titanium 0.017”x0.025” wire springs exerting 0.5N for 1 hour/day for 5 days or 0.8N for 1 hour/day for 10 days [20–22]. For the procedure, mice were anesthetized daily in an isoflurane inhalation induction chamber for the duration of the experiment, weights were monitored daily throughout the experimental procedure. The procedure was documented on the authors IACUC approved protocol.

Tissue Collection and Histomorphometrics:

Adamts5$^{+/+}$ (wild type; WT) and *Adamts5*$^{-/-}$ mouse heads were bisected. The left side of the head was fixed in 4% paraformaldehyde, decalcified in 0.5M EDTA, and processed for histology, Tartrate-Resistant Acid Phosphatase (TRAP) staining or immunohistochemistry (IHC). Safranin O/Fast Green staining was utilized for all histomorphometric analysis.

*Microcomputed tomography (*μCT):

Mineralized cartilage and subchondral bone were analyzed using μCT (SCANCO Medical *ex vivo* uCT40 AG, Brüttisellen, Switzerland). Two-month-old WT and *Adamts5*$^{-/-}$ heads were bisected and the right side of the head and excess tissue was trimmed from the TMJ joint and placed in a 9mm holder. Each sample was scanned in 70% ethanol. Serial tomographic projections were acquired at 70 kV and 114μA, with a voxel size of 6μm and 1000 projections per rotation collected at 300000μs. The DICOM images were transferred, segmented and reconstructed using the AnalyzeDirect/AnalyzePro software (Overland Park, KS). Total volume (TV (mm^3)), bone volume (BV (mm^3)), bone volume fraction (BV/TV (%)), trabecular thickness (TbTh (mm)) and trabecular separation (TbSp (mm)) were determined. The μCT was performed based on a randomly assigned number that blinded the

operator of the scanner and subsequent analysis in the AnalyzeDirect/AnalyzePro software (Overland Park, KS).

Microscopy Quantification:

Sections of *Adamts5*$^{+/+}$ and *Adamts5*$^{-/-}$ mandibular condyles were stained with Safranin O/Fast Green and digital images were acquired with a Zeiss Axio.A1 Microscope (Carl Zeiss Microscopy, Oberkochen, Germany). Cells within the MCC were counted and hypertrophic cells were distinguished by their clear lacunae and red pericellular matrix. Counts represent the average of three serial sections for each mouse analyzed. Amira™ software (Thermo Fisher Scientific) was used to quantify the fibrocartilage volume (voxels) in the mandibular condyle. The quantitative analyses was scored by two lab members that were blinded to genotype.

Immunohistochemistry:

Sections were immunolocalized for Acan (AB1031 Chemicon) and nuclei were stained with propidium iodide (PI). Indirect immunofluorescent digital images were acquired using the Leica TCS SP5 AOBS Confocal Microscope System (Leica Microsystems Inc., Extron, PA). Confocal gain settings were set to a linear range using the most intense fluorescence emission from the tissue sections; the same gain was used to capture digital images of IHC sections within each experiment. Standardized gains settings were used for comparison of normal load (NL) and increased load on the MCC of *Adamts5*$^{+/+}$ and *Adamts5*$^{-/-}$ sections. Sox9 and Acan positive cells were counted and expressed as a percentage of total cells, propidium iodide was used to stain nuclei to quantify total cell number.

Statistical Analysis:

In graphs, each symbol represents data from a single mouse (n=1) for evaluation of the MCC phenotype and each bone parameter obtained by the μCT. The data analyzed in this study are from distinct groups. GraphPad Prism 9 (GraphPad Software Inc.) was utilized to generate graphs. The longest red bar in the center of each group of graphed values represents the mean of the measurements, with smaller red bars above and below the mean indicating the standard deviation. One-way ANOVA was used to calculate the statistical significance between groups for analysis of the hypertrophic zone, Sox9 expression, and hypertrophic Acan positive cells. Adjusted *P* values are indicated for each group comparison with *P* less than 0.05 being significant. In the μCT generated data, the overall ‘global’ *P*-value from the Kruskal-Wallis test was valid, and indicated that there were significant differences among groups. There were 9 pairwise hypothesis tests of interest, and there were 9 separate Kruskal-Wallis tests performed, but only two groups per test were performed (Supplemental appendix). The resulting *P* values were saved, and the false discovery rate (FDR) approach [23] was used to adjust the *P* values for the fact that there were 9 comparisons of interests. The animal numbers were assigned randomly prior to genotyping, this served to blind the investigators at every stage of the study, until the grouping for statistical analysis. To ensure the fidelity of the *Adamts5*$^{-/-}$ homozygous phenotype and to provide littermate controls, animals used in this study were the result of *Adamts5*$^{-/+}$ het X *Adamts5*$^{-/+}$ het matings. The number of mice utilized in this study represents a minimum of eighteen different litters that were required to obtain an appropriate n number for this study.

Results:

Increased TMJ load resulted in a partial rescue of the MCC phenotype of *Adamts5*$^{-/-}$ mice.

Our previous studies indicate that the mandibular condyle of *Adamts5*$^{-/-}$ mice exhibits significant differences in the MCC [16] and trabecular bone compared to *Adamts5*$^{+/+}$ [17]. To determine if changes in the *Adamts5*$^{-/-}$ mandibular condyle due to loss of ADAMTS5 in development, results in an altered response to increased load, a forced mouth open assay was performed. An orthodontic spring was placed in the open mouth of mice with a force and duration of either 0.5 N for 1 hour for 5 days (0.5N/5d) or 0.8N for 1 hour for 10 days (0.8N/10d) (Fig. 1A) [20–22]. Under normal load (NL, i.e. baseline) *Adamts5*$^{-/-}$ mice exhibit pathological changes in the zonal architecture of the MCC, [16] (Fig. 1B, E). In the *Adamts5*$^{+/+}$ MCC under NL, the different zones are readily identified by their distinctive cell morphology as well as surrounding ECM (red-Safranin O, green-Fast Green). However, in *Adamts5*$^{-/-}$ mice, the zones are significantly altered by expansion of the proliferative layer (yellow bar, Fig. 1B, E) and reduction of the hypertrophic layer (green bar, Fig. 1B, E, H). In addition, the MCC of *Adamts5*$^{-/-}$ mice exhibit red staining in the proliferative zone which stains green in the *Adamts5*$^{+/+}$ MCC (Fig. 1B, E). Given the changes in the zones of the MCC at NL, we hypothesized that increased load may differentially affect the *Adamts5*$^{+/+}$ MCC and *Adamts5*$^{-/-}$ MCC.

In response to 0.8N/10d increased load, the hypertrophic layer of the *Adamts5*$^{-/-}$ MCC was significantly increased compared to *Adamts5*$^{-/-}$ mice with NL (Fig. 1H; n=17; P=0.007) (Fig. 1E, G, H; green bar). There was also a significant reduction in overall cartilage thickness in the *Adamts5*$^{-/-}$ mice subjected to 0.8N/10d increased load compared to NL (Fig. 1I; (n=17). In fact, with 0.8N/10d increased load the hypertrophic layer in the *Adamts5*$^{-/-}$ MCC was not significantly different from the *Adamts5*$^{+/+}$ MCC (Fig. 1D, G, H; n=6), suggesting increased load resulted in an apparent rescue of the hypertrophic zone thickness in the *Adamts5*$^{-/-}$ MCC. The increase in hypertrophic layer of the *Adamts5*$^{-/-}$ MCC subjected to increased load was not due to an increase in MCC cells (Fig. 1J).

The chondrogenic programing due to increased load is reduced in the *Adamts5*$^{-/-}$ MCC compared to *Adamts5*$^{+/+}$.

To determine the extent to which increased load impacted chondrogenic signaling, expression of the essential cartilage factor SRY-box transcription factor 9, (Sox9) was evaluated. Increased load resulted in a significant increase in Sox9 positive cells in the *Adamts5*$^{+/+}$ MCC (n=4) compared to NL (Fig. 2A, B, E); the expression pattern of Sox9 in the *Adamts5*$^{+/+}$ MCC expanded to the upper proliferative layer that is generally devoid of Sox9 under NL (n=5) (Fig. 2A, B; green arrows). Mice deficient in ADAMTS5 did not exhibit a significant difference in Sox9 expression with increased load (n=5) compared to NL (n=4) (Fig. 2C, D, E) indicating the ability of increased load to enhance Sox9 chondrogenic signaling was blunted by ADAMTS5 deficiency.

The expression and localization of Acan, the major cartilage proteoglycan and a substrate of ADAMTS5 was also evaluated. Our previous work indicated that without ADAMTS5, Acan accumulated within the upper proliferative zone of the MCC, (Fig. 2H; yellow asterisk),

compared to *Adamts5*$^{+/+}$ (Fig. 2F) [16]. The *Adamts5*$^{+/+}$ MCC hypertrophic chondrocytes also exhibit an Acan positive pericellular matrix (n=6) which is virtually lost in *Adamts5*$^{-/-}$ mice with NL (n=9) (Fig. 2F, H) [16]. However, increased load on the *Adamts5*$^{-/-}$ MCC (n=12) resulted in a significant increase in Acan positive hypertrophic chondrocytes compared to *Adamts5*$^{-/-}$ mice with NL (Fig. 2F–J; $P<.007$). In the *Adamts5*$^{-/-}$ MCC with increased load there were still significantly fewer Acan positive hypertrophic chondrocytes compared to *Adamts5*$^{+/+}$ MCC with increased load. Hypertrophic chondrocytes that were Acan positive were also evident in the upper proliferative zone in *Adamts5*$^{+/+}$ mice with increased load (Fig. 2G; green arrows) and correlated with Sox9 expression (Fig. 2B) whereas *Adamts5*$^{-/-}$ mice with NL did not exhibit Acan or Sox9 positive cells in the upper fibrocartilage zones.

Microcomputed tomography indicates the trabeculated bone of the mandibular condylar in *Adamts5*$^{-/-}$ mice exhibited significantly less adaptations to increased TMJ load than *Adamts5*$^{+/+}$ mice.

μCT was used to analyze the trabecular bone of mandibular condyles from *Adamts5*$^{+/+}$ (+/+, n=38) and *Adamts5*$^{-/-}$ mice (−/−, n=27) under NL, increased load 0.5N/5d (+/+, n=18; −/−, n=19) or increased load 0.8N/10d (+/+, n=18; −/−, n=17). The graphs on the left side indicate the changes of each animal in each independent group (Fig. 3A, C, E, G, I). Since the bone parameters are different with NL between *Adamts5*$^{+/+}$ and *Adamts5*$^{-/-}$ mandibular condyles, graphs on the right (Fig. 3B, D, F, H, J) highlight the mean percentage change of each μCT parameter from NL to increased load (0.5NL/5d and 0.8N/10d). The slope of the lines depicts the increase or decrease and percentage change from NL.

As previously published, the TV is significantly different between genotypes at NL (i.e., baseline) (Fig. 3A)[17]. While increased load resulted in a significant reduction of TV in the *Adamts5*$^{+/+}$ mandibular condyle, there was no significant change in the *Adamts5*$^{-/-}$ (Fig. 3A). Note that the TV in each of the load groups was significantly reduced in the *Adamts5*$^{+/+}$ compared to the corresponding load group in *Adamts5*$^{-/-}$ mandibular condyles. The graph (Fig. 3B) depicts the TV changes in each genotype with increased load in comparison to the differences at NL. In the *Adamts5*$^{+/+}$ mice there was a significant 13.89% reduction in TV while increased load did not significantly alter the TV in the *Adamts5*$^{-/-}$ mandibular condyles compared to NL.

There was also a significant difference in the BV between genotypes in NL conditions. However, increased load resulted in a significant reduction in BV in the *Adamts5*$^{+/+}$ mandibular condyles compared to the *Adamts5*$^{-/-}$ mandibular condyles that were not significantly reduced compared to NL (Fig. 3C). The *Adamts5*$^{+/+}$ mice experienced an average of 20.2% reduction in BV mean due to increased load, while the mandibular condyles of the *Adamts5*$^{-/-}$ mice did not exhibit a significant BV change (Fig. 3D).

The BV/TV (referred to as bone volume fraction) in the mandibular condyles of the *Adamts5*$^{-/-}$ mice compared to *Adamts5*$^{+/+}$ mice was significantly reduced at NL [16]. Here we observed that increased load significantly reduced the BV/TV in the *Adamts5*$^{+/+}$ and *Adamts5*$^{-/-}$ TMJ (Fig. 3E). The reduction in mean BV/TV was similar between genotypes (*Adamts5*$^{+/+}$, 7.55% and *Adamts*5$^{-/-}$7.02%) (Fig. 3F). The adverse BV/TV reduction was

significant in each of the comparable load groups between *Adamts5*$^{+/+}$ and *Adamts5*$^{-/-}$ genotypes. The BV/TV was the most severely reduced in the *Adamts5*$^{-/-}$ mandibular condyles with increased 0.8N/10d load, compared to any other group suggestive of adverse bone remodeling. Although neither the TV or BV was significantly affected by increased load in the *Adamts5*$^{-/-}$ mandibular condyles, the trend of an increase in TV and a decrease in BV significantly reduced the BV/TV in *Adamts5*$^{-/-}$ mandibular condyles.

TbTh in the mandibular condyle of *Adamts5*$^{-/-}$ mice is significantly reduced compared to *Adamts5*$^{+/+}$ under NL (P<.05) (Fig. 3G, H) [16]. With increased TMJ load there was a significant reduction in TbTh in the *Adamts5*$^{+/+}$ mice, which resulted in significant differences between genotypes among comparable load groups. However the TbTh of the mandibular condyle in the *Adamts5*$^{-/-}$ mice was not significantly changed by increased load.

In NL the TbSp in the mandibular condyle of the TMJ is significantly increased in the *Adamts5*$^{-/-}$ mice compared to *Adamts5*$^{+/+}$ [16]. However, the increase in load in the *Adamts5*$^{+/+}$ significantly increased the TbSp in the mandibular condyle but the changes in mean TbSp were not significant between any of the *Adamts5*$^{-/-}$ mice load groups. These data indicated that the *Adamts5*$^{+/+}$ mandibular condyles responded to changes in load by increasing their TbSp, while the *Adamts5*$^{-/-}$ mice were not significantly responsive (Fig. 3G, H). Collectively μCT revealed that the mandibular condyles of *Adamts5*$^{-/-}$ mice were less responsive to changes in increased load compared to *Adamts5*$^{+/+}$.

TRAP positivity dramatically increased in the mandibular condyles of the *Adamts5*$^{-/-}$ mice with 0.8N/10d increased load compared to *Adamts5*$^{+/+}$.

Since there was a reduction in the BV/TV in the *Adamts5*$^{-/-}$ mice with increased load, Tartrate Resistance Acid Phosphatase activity (TRAP) staining, used to indicate osteoclasts, was performed on *Adamts5*$^{+/+}$ NL (n=4), *Adamts5*$^{+/+}$ 0.8N/10d increased load (n=6) as well as *Adamts5*$^{-/-}$ NL (n=9) and *Adamts5*$^{-/-}$ 0.8N/10d increased load (n=18). TRAP staining revealed a significant increase in the *Adamts5*$^{-/-}$ 0.8N/10d increased load group compared to *Adamts5*$^{-/-}$ with normal load (Fig. 4; P<.001) and *Adamts5*$^{+/+}$ with increased load (P<.01).

Discussion

Increased load on the TMJ enhanced cartilage programming in the MCC but this shift in pro-cartilage expression was reduced in *Adamts5*$^{-/-}$ mice compared to *Adamts5*$^{+/+}$. The partial restoration of zonal organization in response to increased load in *Adamts5*$^{-/-}$ MCC indicated that other factors may be upregulated by increased load to enhance chondrogenesis, but cannot fully compensate for the loss of ADAMTS5. Since mature hypertrophic chondrocytes express the proteoglycan proteases, ADAMTS1, MMP9, and MMP13, [17] there is the potential of feed forward signaling with increased load in the MCC, where the increase in hypertrophic chondrocytes results in expression of additional ECM proteases that promote proteoglycan remodeling in the cartilage ECM.

Previous studies indicated that a consequence of increased load on the mandibular condyle is increased chondrogenesis [20–22]. In this study expression of Sox9, a marker of

chondrocytes [24 and a critical factor that directly regulates the production of cartilage ECM {Bell, 1997 #7593, 25, 26] was significantly different in the MCC of *Adamts5*$^{-/-}$ and *Adamts5*$^{+/+}$ with and without increased load. Our published study indicated that loss of ADAMTS5 resulted in a significant decrease in Sox9 expression that translated into reduction of the MCC hypertrophic zone [16]. In the developing and adult mandibular condyle with NL, Sox9 expression localizes to the chondrogenic and hypertrophic cartilage zones. In contrast, ADAMTS5 is expressed most prominently within the proliferative zone of the MCC, rich in Collagen I, fibrous ECM [16]. Based on published work [16, 17] and results in this study, ADAMTS5 activity may be critical for crosstalk between the MCC zones to regulate chondrogenesis and to promote adaptability of the TMJ. However, understanding the intersection of Sox9, ADAMTS5 and Acan turnover in fibrocartilage will require additional experimentation.

One of the unique aspects of the mandibular condyle is that a majority of hypertrophic chondrocytes dedifferentiate and are reprogramed into bone forming cells [27–31]. Our previous study indicates that ADAMTS5 is strongly expressed in the de-differentiated hypertrophic chondrocytes and that loss of ADAMTS5 results in a reduction of bone-forming cells [17]. Although increased load on the *Adamts5*$^{-/-}$ mandibular condyle resulted in an increase in hypertrophic chondrocytes which could be interpreted as a partial rescue of the chondrogenic MCC phenotype, increased load was detrimental to the underlying subchondral bone. The subchondral bone of the *Adamts5*$^{+/+}$ mandibular condyle was more responsive to increased load than the *Adamts5*$^{-/-}$. The TV, BV, BV/TV, TbTh and TbSp were all significantly changed with increased load on the *Adamts5*$^{+/+}$ mandibular condyle while the *Adamts5*$^{-/-}$ was only significantly altered in the BV/TV but exhibited a dramatic reduction in bone volume fraction. Collectively, these data may suggest that ADAMTS5 is essential for the coordinated process of chondrogenesis and osteogenesis and loss of ADAMTS5 may significantly reduce the ability of the trabeculated bone of the mandibular condyle to increased load.

ADAMTS5 is regulated in well-established mechanotransductive pathways that alter ECM composition. For example, Indian hedgehog (Ihh) is a key regulator of hypertrophic chondrogenic differentiation [32] and is present within primary cilia [33] that detect changes in biomechanical forces. Conditional deletion of an essential cilia transport gene, Intraflagellar Transport 88, (*Ift88*) inhibits Ihh and results in elevated levels of ADAMTS5 [34]. Ihh also binds directly to chondroitin sulfate sidechains of Acan, indicating the potential for ADAMTS5 cleavage of Acan to release Ihh signaling molecules for pathway activation [35]. Loss of chondrocytes expressing differentiation factors Ihh and collagen type X alpha 1 chain (Col10a1), is also associated with induction of Wnt signaling in the developing MCC [36]. We have shown that ADAMTS5 deficient mice exhibit a reduction of Col10 in the MCC [16]. Furthermore, expression of Col10a1, a Wnt/beta catenin pathway gene, requires ADAMTS5 activity in a surgically induced model of knee osteoarthritis [37]. When *Axin1,* a regulator of Wnt signaling, is excised from Acan-expressing chondrocytes (Axin1^{Agc1ER}), *Adamts5* expression is upregulated [38]. Upregulation of *Adamts5* in the mandibular condyle is also promoted by the over-expression of the canonical Wnt signaling factor beta catenin [39]. Therefore, ADAMTS5 may be involved in multiple mechanotransductive pathways in response to changes in TMJ load.

A primary limitation of the forced open mouth increased load model is that it utilizes static load; a more dynamic approach to altered load would complement data obtained in this study. For example, use of the unilateral anterior crossbite prosthesis and subsequent replacement with bilateral anterior elevation prosthesis is a dynamic approach to degenerative and then rehabilitative responses to load [40–43]. Soft diet with incisor trimming is another dynamic approach that would be effective in elucidating the role of ADAMTS5 to adaptive remodeling and complement the increased load approach utilized in this study [44]. In this study we have analyzed the response to increased load on the mandibular condyles between *Adamts5*$^{+/+}$ and *Adamts5*$^{-/-}$ which exhibit differences in their μCT under NL. An additional experiment where *Adamts5* is deleted at the onset of increased TMJ load would specifically focus on the role of ADAMTS5 in adaptation of the joint to increased load, independent of the MCC and trabecular bone alterations that are generated during development in ADAMTS5 global knockout mice, as used in this study. Another point of consideration is that the expected range of adaptability required to maintain healthy TMJ fibrocartilage in mouse models is unclear. The pathological remodeling observed in wild type mice in response to increased load may indicate that the applied force chosen for this study simulates pathological load on the TMJ meaning it is outside the normal range of biomechanical forces that these animals encounter in their natural environment.

In the TMJ, the adaptation to increased load involves both the chondrogenesis of the MCC as well as remodeling of the adjacent subchondral bone. The observation that increased load enhanced the hypertrophic chondrocytes may indicate that fewer hypertrophic chondrocytes dedifferentiate into bone forming cells when the mandibular condyle is under increased load. Data from this work as well as others [16] [39] [38] place ADAMTS5 in a pivotal role of TMJ remodeling. Additional studies are needed to address how ADAMTS5 proteolytically cleaved ECM substrates may be involved in TMJ mechanotransduction and elucidation of their requirement for regenerative therapy approaches to TMJ diseases in the human population.

Supplementary Material

Refer to Web version on PubMed Central for supplementary material.

Acknowledgments:

The authors would like to thank Dr. Paul Nietert for his contribution of statistical analysis. Dr Nietert is supported, in part, by the National Center for Advancing Translational Sciences of the National Institutes of Health under Grant Number UL1 TR001450. The content is solely the responsibility of the authors and does not necessarily represent the official views of the National Institutes of Health.

Funding:

NIH, NHLBI HL 160802 (CBK), American Heart Association #17GRNT33700214 (CBK), NIH, NHLBI HL121382 (CBK), T32 DE017551 (SCP, ARD), F30 1F30DEO28180 (ARD).

ABBREVIATIONS:

TMJ	Temporomandibular Joint
MCC	Mandibular condylar cartilage

ECM	extracellular matrix
ADAMTS5	A Disintegrin And Metalloproteinase with ThromboSpondin Motifs (ADAMTSs)
TMJ-OA	TMJ osteoarthritis (TMJOA)
Acan	Aggrecan
NL	normal load
TV	Total volume
BV	bone volume
BV/TV	bone volume fraction
TbTh	trabecular thickness
TbSp	trabecular separation
μCT	Microcomputed topography

References

1. Wang XD, Zhang JN, Gan YH, Zhou YH. Current understanding of pathogenesis and treatment of TMJ osteoarthritis. J Dent Res 2015; 94: 666–673. [PubMed: 25744069]
2. Zhang J, Jiao K, Zhang M, Zhou T, Liu XD, Yu SB, et al. Occlusal effects on longitudinal bone alterations of the temporomandibular joint. J Dent Res 2013; 92: 253–259. [PubMed: 23340211]
3. Milam SB. Pathogenesis of degenerative temporomandibular joint arthritides. Odontology 2005; 93: 7–15. [PubMed: 16170470]
4. Zarb GA, Carlsson GE. Temporomandibular disorders: osteoarthritis. J Orofac Pain 1999; 13: 295–306. [PubMed: 10823044]
5. Robinson J, O'Brien A, Chen J, Wadhwa S. Progenitor Cells of the Mandibular Condylar Cartilage. Curr Mol Biol Rep 2015; 1: 110–114. [PubMed: 26500836]
6. Mizoguchi I, Toriya N, Nakao Y. Growth of the manddible and biological characteristics of the mandibular condylar cartilage. Japanese Dental Science Review 2013; 49: 139–150.
7. Shibukawa Y, Young B, Wu C, Yamada S, Long F, Pacifici M, et al. Temporomandibular joint formation and condyle growth require Indian hedgehog signaling. Dev Dyn 2007; 236: 426–434. [PubMed: 17191253]
8. Little CB, Meeker CT, Golub SB, Lawlor KE, Farmer PJ, Smith SM, et al. Blocking aggrecanase cleavage in the aggrecan interglobular domain abrogates cartilage erosion and promotes cartilage repair. J Clin Invest 2007; 117: 1627–1636. [PubMed: 17510707]
9. Wang K, Xu J, Hunter DJ, Ding C. Investigational drugs for the treatment of osteoarthritis. Expert Opin Investig Drugs 2015: 1–18.
10. Dancevic CM, McCulloch DR. Current and emerging therapeutic strategies for preventing inflammation and aggrecanase-mediated cartilage destruction in arthritis. Arthritis Res Ther 2014; 16: 429. [PubMed: 25606593]
11. Sophia Fox AJ, Bedi A, Rodeo SA. The basic science of articular cartilage: structure, composition, and function. Sports Health 2009; 1: 461–468. [PubMed: 23015907]
12. Kiani C, Chen L, Wu YJ, Yee AJ, Yang BB. Structure and function of aggrecan. Cell Res 2002; 12: 19–32. [PubMed: 11942407]
13. Wang M, Li S, Xie W, Shen J, Im HJ, Holz JD, et al. Activation of beta-catenin signalling leads to temporomandibular joint defects. Eur Cell Mater 2014; 28: 223–235. [PubMed: 25340802]

14. Kintakas C, McCulloch DR. Emerging roles for ADAMTS5 during development and disease. Matrix Biol 2011; 30: 311–317. [PubMed: 21683141]
15. Stanton H, Rogerson FM, East CJ, Golub SB, Lawlor KE, Meeker CT, et al. ADAMTS5 is the major aggrecanase in mouse cartilage in vivo and in vitro. Nature 2005; 434: 648–652. [PubMed: 15800625]
16. Rogers AW, Cisewski SE, Kern CB. The Zonal Architecture of the Mandibular Condyle Requires ADAMTS5. J Dent Res 2018; 97: 1383–1390. [PubMed: 29879379]
17. Rogers-DeCotes AW, Porto SC, Dupuis LE, Kern CB. ADAMTS5 is required for normal trabeculated bone development in the mandibular condyle. Osteoarthritis Cartilage 2021; 29: 547–557. [PubMed: 33561540]
18. Jungers KA, Le Goff C, Somerville RP, Apte SS. Adamts9 is widely expressed during mouse embryo development. Gene Expr Patterns 2005; 5: 609–617. [PubMed: 15939373]
19. McCulloch DR, Nelson CM, Dixon LJ, Silver DL, Wylie JD, Lindner V, et al. ADAMTS metalloproteases generate active versican fragments that regulate interdigital web regression. Dev Cell 2009; 17: 687–698. [PubMed: 19922873]
20. Sobue T, Yeh WC, Chhibber A, Utreja A, Diaz-Doran V, Adams D, et al. Murine TMJ loading causes increased proliferation and chondrocyte maturation. J Dent Res 2011; 90: 512–516. [PubMed: 21248355]
21. Fujisawa T, Kuboki T, Kasai T, Sonoyama W, Kojima S, Uehara J, et al. A repetitive, steady mouth opening induced an osteoarthritis-like lesion in the rabbit temporomandibular joint. J Dent Res 2003; 82: 731–735. [PubMed: 12939359]
22. Utreja A, Dyment NA, Yadav S, Villa MM, Li Y, Jiang X, et al. Cell and matrix response of temporomandibular cartilage to mechanical loading. Osteoarthritis Cartilage 2016; 24: 335–344. [PubMed: 26362410]
23. Benjamini Y, Hochberg Y. Controlling the false discovery rate: a practical and powerful approach to multiple testing. Journal of the Royal Statistical Methodology Series B 1995; 57: 11.
24. Akiyama H, Lyons JP, Mori-Akiyama Y, Yang X, Zhang R, Zhang Z, et al. Interactions between Sox9 and beta-catenin control chondrocyte differentiation. Genes Dev 2004; 18: 1072–1087. [PubMed: 15132997]
25. Ng LJ, Wheatley S, Muscat GE, Conway-Campbell J, Bowles J, Wright E, et al. SOX9 binds DNA, activates transcription, and coexpresses with type II collagen during chondrogenesis in the mouse. Dev Biol 1997; 183: 108–121. [PubMed: 9119111]
26. Zhou G, Lefebvre V, Zhang Z, Eberspaecher H, de Crombrugghe B. Three high mobility grouplike sequences within a 48-base pair enhancer of the Col2a1 gene are required for cartilage-specific expression in vivo. J Biol Chem 1998; 273: 14989–14997.
27. Hinton RJ, Jing Y, Jing J, Feng JQ. Roles of Chondrocytes in Endochondral Bone Formation and Fracture Repair. J Dent Res 2017; 96: 23–30. [PubMed: 27664203]
28. Jing Y, Zhou X, Han X, Jing J, von der Mark K, Wang J, et al. Chondrocytes Directly Transform into Bone Cells in Mandibular Condyle Growth. J Dent Res 2015; 94: 1668–1675. [PubMed: 26341973]
29. Zhou X, von der Mark K, Henry S, Norton W, Adams H, de Crombrugghe B. Chondrocytes transdifferentiate into osteoblasts in endochondral bone during development, postnatal growth and fracture healing in mice. PLoS Genet 2014; 10: e1004820.
30. Yang G, Zhu L, Hou N, Lan Y, Wu XM, Zhou B, et al. Osteogenic fate of hypertrophic chondrocytes. Cell Res 2014; 24: 1266–1269. [PubMed: 25145361]
31. Yang L, Tsang KY, Tang HC, Chan D, Cheah KS. Hypertrophic chondrocytes can become osteoblasts and osteocytes in endochondral bone formation. Proc Natl Acad Sci U S A 2014; 111: 12097–12102.
32. Kronenberg HM. Developmental regulation of the growth plate. Nature 2003; 423: 332–336. [PubMed: 12748651]
33. Marshall WF. Basal bodies platforms for building cilia. Curr Top Dev Biol 2008; 85: 1–22. [PubMed: 19147000]

34. Haycraft CJ, Zhang Q, Song B, Jackson WS, Detloff PJ, Serra R, et al. Intraflagellar transport is essential for endochondral bone formation. Development 2007; 134: 307–316. [PubMed: 17166921]

35. Cortes M, Baria AT, Schwartz NB. Sulfation of chondroitin sulfate proteoglycans is necessary for proper Indian hedgehog signaling in the developing growth plate. Development 2009; 136: 1697–1706. [PubMed: 19369399]

36. Tamamura Y, Otani T, Kanatani N, Koyama E, Kitagaki J, Komori T, et al. Developmental regulation of Wnt/beta-catenin signals is required for growth plate assembly, cartilage integrity, and endochondral ossification. J Biol Chem 2005; 280: 19185–19195.

37. Bateman JF, Rowley L, Belluoccio D, Chan B, Bell K, Fosang AJ, et al. Transcriptomics of wild-type mice and mice lacking ADAMTS-5 activity identifies genes involved in osteoarthritis initiation and cartilage destruction. Arthritis Rheum 2013; 65: 1547–1560. [PubMed: 23436205]

38. Zhou Y, Shu B, Xie R, Huang J, Zheng L, Zhou X, et al. Deletion of Axin1 in condylar chondrocytes leads to osteoarthritis-like phenotype in temporomandibular joint via activation of beta-catenin and FGF signaling. J Cell Physiol 2019; 234: 1720–1729. [PubMed: 30070692]

39. Hui T, Zhou Y, Wang T, Li J, Zhang S, Liao L, et al. Activation of beta-catenin signaling in aggrecan-expressing cells in temporomandibular joint causes osteoarthritis-like defects. Int J Oral Sci 2018; 10: 13. [PubMed: 29686224]

40. Jiao K, Niu LN, Wang MQ, Dai J, Yu SB, Liu XD, et al. Subchondral bone loss following orthodontically induced cartilage degradation in the mandibular condyles of rats. Bone 2011; 48: 362–371. [PubMed: 20850574]

41. Wang YL, Zhang J, Zhang M, Lu L, Wang X, Guo M, et al. Cartilage degradation in temporomandibular joint induced by unilateral anterior crossbite prosthesis. Oral Dis 2014; 20: 301–306. [PubMed: 23614573]

42. Wang D, Yang H, Zhang M, Zhang H, Lu L, Zhang J, et al. Insulin-like growth factor-1 engaged in the mandibular condylar cartilage degeneration induced by experimental unilateral anterior crossbite. Arch Oral Biol 2019; 98: 17–25. [PubMed: 30419485]

43. Shibata S, Suzuki S, Tengan T, Yamashita Y. A histochemical study of apoptosis in the reduced ameloblasts of erupting mouse molars. Arch Oral Biol 1995; 40: 677–680. [PubMed: 7575241]

44. Chen J, Sobue T, Utreja A, Kalajzic Z, Xu M, Kilts T, et al. Sex differences in chondrocyte maturation in the mandibular condyle from a decreased occlusal loading model. Calcif Tissue Int 2011; 89: 123–129. [PubMed: 21597908]

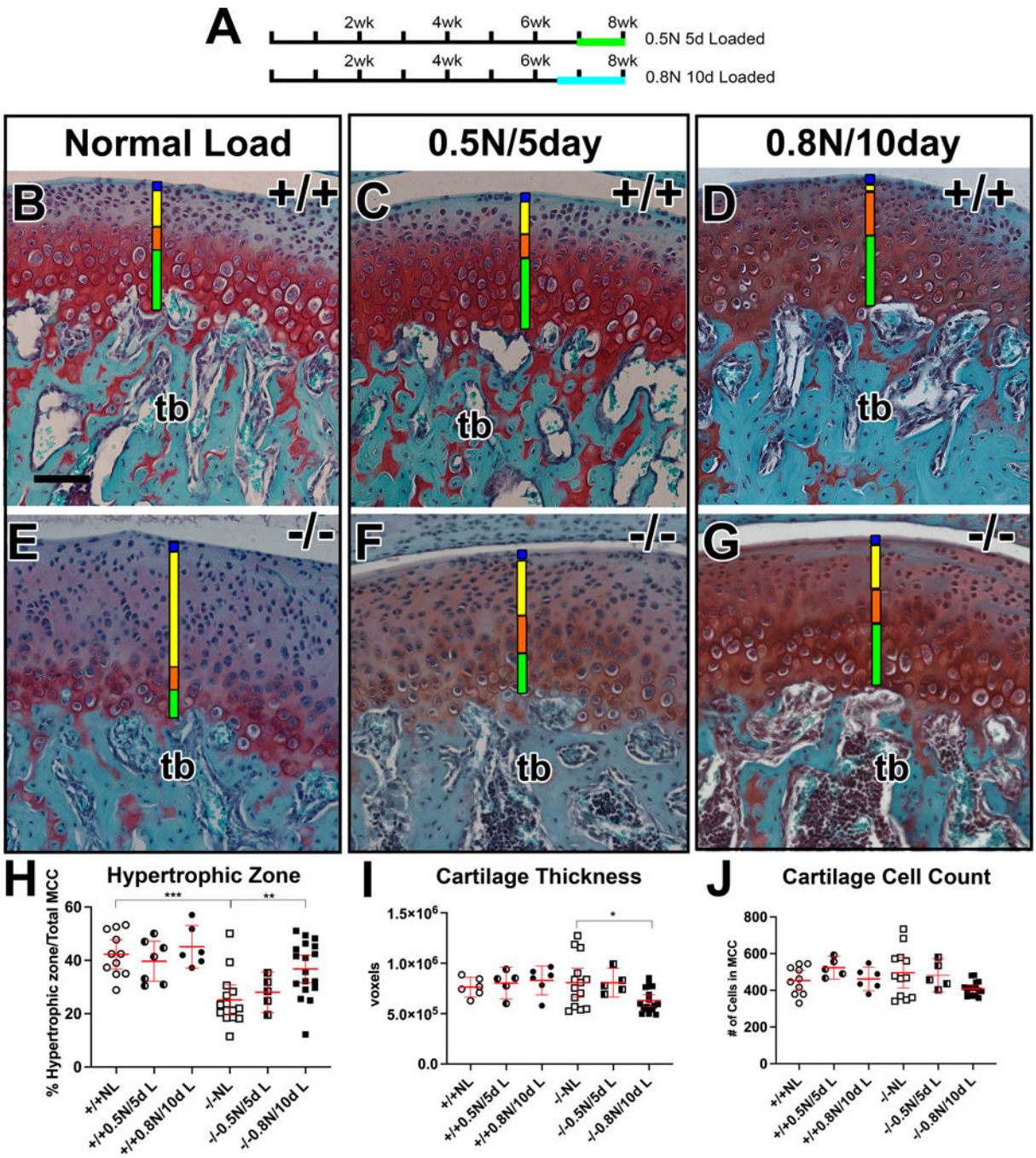

Figure 1: Increased TMJ load resulted in a partial rescue of the MCC zonal organization in *Adamts5*$^{-/-}$ mice.

Timeline of study design and exposure to increased load (A). Duration of 0.5N 5 day study (0.5N/5d, green line); 0.8N 10 day study (0.8N/10d, cyan line). Safranin O stained sections of the developing condyle 8 week old *Adamts5*$^{+/+}$ (+/+; B-D) and *Adamts5*$^{-/-}$ (−/−; E-G). Normal load (NL; B, E), increased load 0.5N/5d, (D, F) and increased load, 0.8N/10d (D, G). Green bars (B-G) hypertrophic zone, orange bars-chondrocytic zone, yellow bars-polymorphic zone; blue bars-superficial zone; tb-trabecular bone. Bar in B =100μm, applies to C-G. Graph (H) indicates % hypertrophic zone/total MCC in *Adamts5*$^{+/+}$ NL

(open circles), *Adamts5*$^{+/+}$ 0.5N/5d (half circles), *Adamts5*$^{+/+}$ 0.8N/10d (closed circles), *Adamts5*$^{-/-}$ NL (open squares) *Adamts5*$^{-/-}$ 0.5N/5d (half squares), *Adamts5*$^{-/-}$ 0.8N/10d (closed squares) ***-P <0.001; **-P =0.007; Graph (I) cartilage thickness measured in voxels *-P<0.05. and graph (J) total cell count in the MCC. Each point on the graph indicates data from one mouse. Middle red bars on each graph represent the average of the mean with the smaller upper and lower red bars indicating the standard deviation.

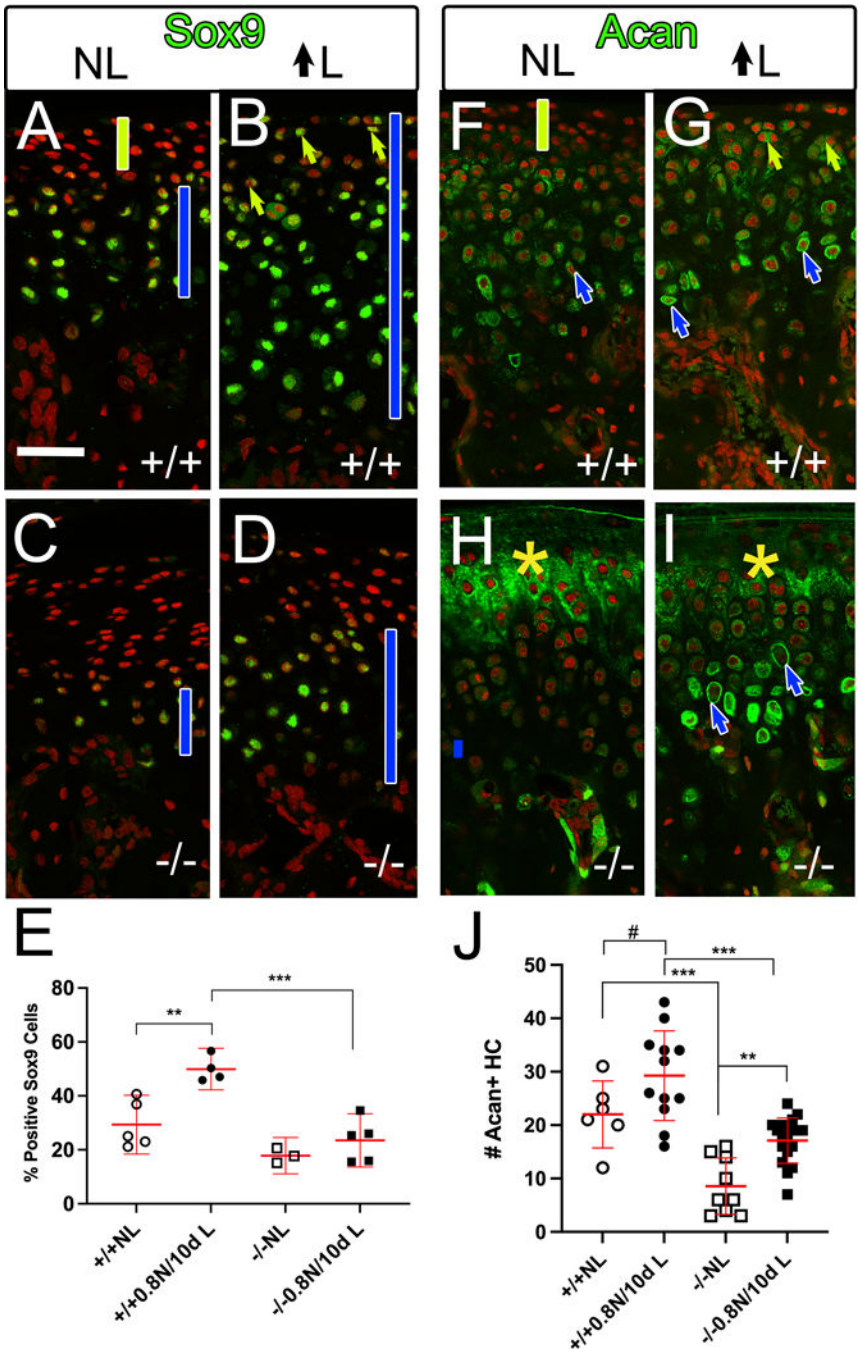

Figure 2: The response of chondrogenesis in the *Adamts5*$^{-/-}$ mandibular condylar cartilage to increased load was not as robust as *Adamts5*$^{+/+}$.

Immunolocalized sections of 8 week old MCC from *Adamts5*$^{+/+}$ (+/+; A, B, F, G) and *Adamts5*$^{-/-}$ (−/−; C, D, H, I) under normal load (NL; A, C, F, H), and increased load, 0.8N 10 day (⬆L; B, D, G, I). Sox9 immunolocalization (Green, A-D); red- propidium iodide to highlight nuclei (A-I). Blue lines (A-D) zones of Sox9 positive expression. Green bar (A) region negative for Sox9 in NL becomes positive for Sox9 with increased load (B, green arrows). White Bar in A =50μm, applies to B-I. Quantification of % positive Sox9 cells (E). Immunolocalization of Acan (F, G, H, I). Green bar (F) region negative for Acan in

NL becomes positive for Acan with increased load (G, green arrows). Blue arrows (F, G, I) pericellular Acan in chondrocytes. Yellow asterisks (H, I) extracellular accumulation of Acan in upper zones of *Adamts5*$^{-/-}$ MCC. Quantification of Acan positive hypertrophic chondrocytes (J). Graphs (E, J); *Adamts5*$^{+/+}$ NL (open circle), *Adamts5*$^{+/+}$ 0.8N/10d (closed circle), *Adamts5*$^{-/-}$ NL (open squares), *Adamts5*$^{-/-}$ 0.8N/10d (closed squares). Each point on the graph indicates data from one mouse. Middle red bars represent the average of the mean with the smaller upper and lower red bars indicating the standard deviation. Graph (E) **-*P*.0038, ***-*P* =.0004; (J) #-*P* =.095, ***-*P* <.001, **-*P* =.007.

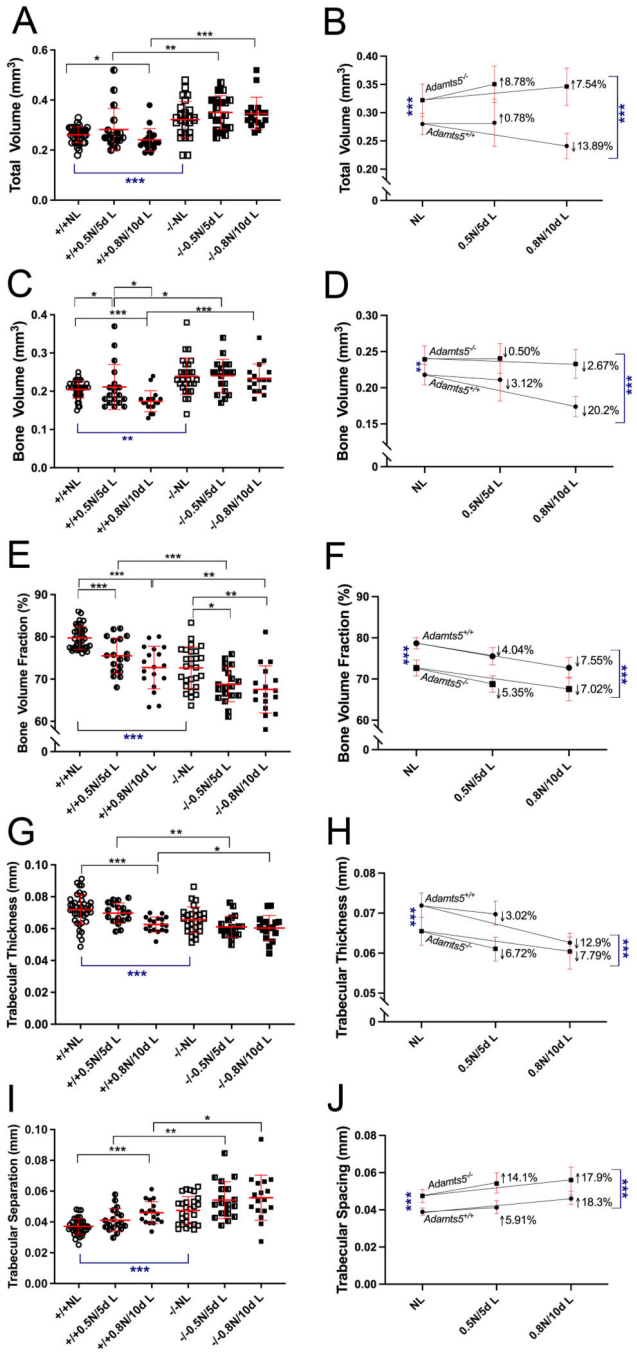

Figure 3: Microtomography indicates the trabeculated bone of the mandibular condylar in *Adamts5*$^{-/-}$ mice exhibited significantly less adaptations to increased TMJ load than *Adamts5*$^{+/+}$ mice.

μCT of mandibular condyles from *Adamts5*$^{+/+}$ NL (open circles) *Adamts5*$^{+/+}$ 0.5N/5d (half circles), *Adamts5*$^{+/+}$ 0.8N/10d (closed circles), *Adamts5*$^{-/-}$ NL (open squares) *Adamts5*$^{-/-}$ 0.5N/5d (half squares), *Adamts5*$^{-/-}$ 0.8N/10d (closed squares). Graphs of Total Volume (TV; A), Bone Volume (BV; C), Bone Volume Fraction (BV/TV; E) Trabecular Thickness (TbTh; G) and Trabecular Separation (TbSp; L) are shown. Each point on the graphs (A, C, E, G, I) represents measurements from one condyle. The blue bars at the bottom of the symbols on

the graphs (A, C, E, G, I) denote the differences in NL between genotypes. Right side graphs (B, D, F, H, J) indicate the percent change of μCT parameters in each genotype from NL, to 0.5N/5d and NL to 0.8N/10d. The blue asterisks on the right graphs (B, D, F, H, J) indicate the differences between genotypes at NL and with 0.8N/10d increased load. *P <.05, ** P <.01; ***P <.001. Middle red bars represent the average of the mean with the smaller upper and lower red bars indicating the standard deviation.

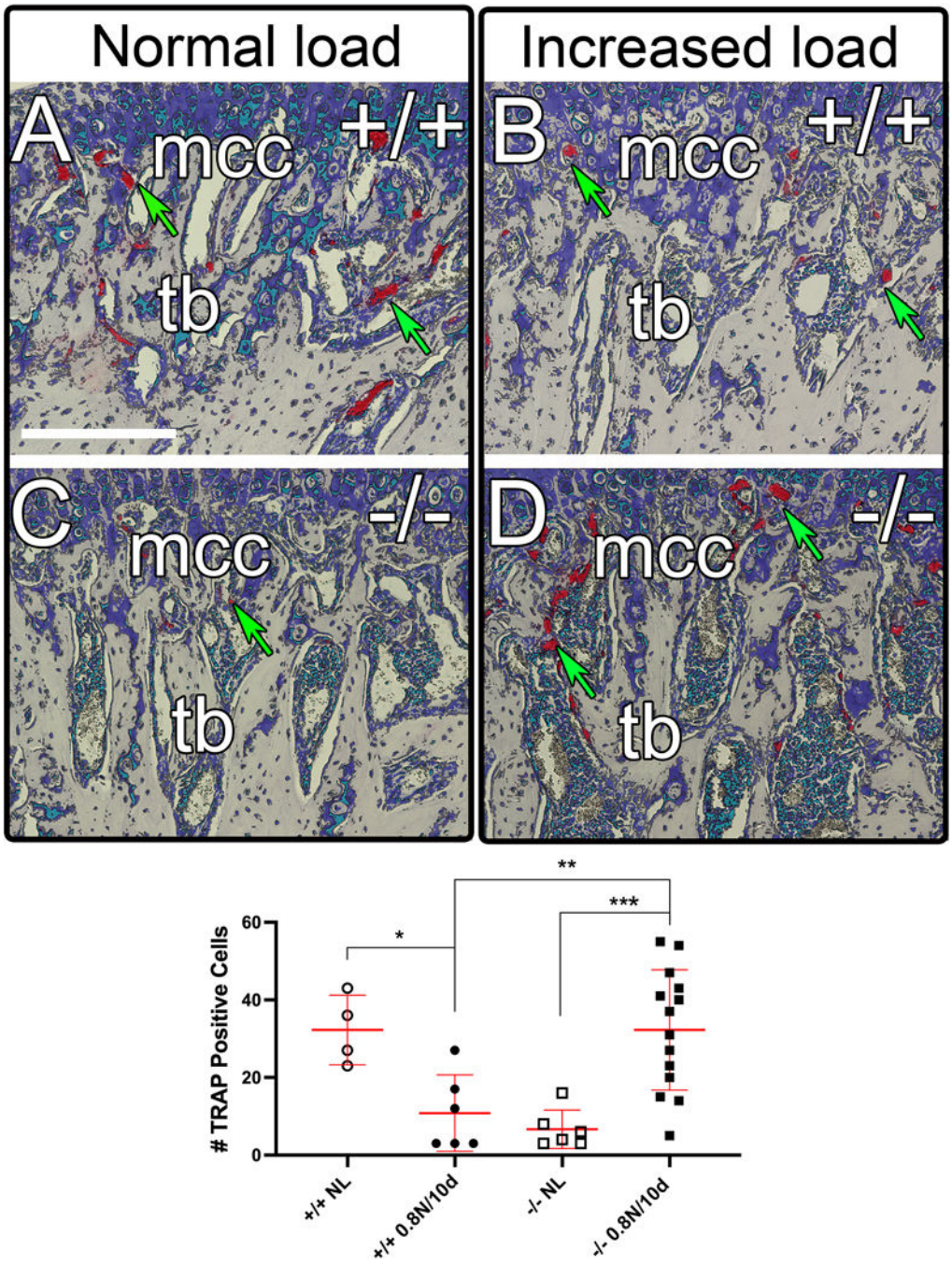

Figure 4: Increased load on the *Adamts5*$^{-/-}$ TMJ significantly increases the number of TRAP positive osteoclasts in the mandibular condyle compared to *Adamts5*$^{+/+}$.

Sections of TRAP staining from the mandibular condyle of 8 week old *Adamts5*$^{+/+}$ NL (A), *Adamts5*$^{+/+}$ 0.8N/10d (B), *Adamts5*$^{-/-}$ NL (C) and *Adamts5*$^{-/-}$ 0.8N/10d (D). Green arrows (A-D) indicate examples of TRAP positive cells. mcc-mandibular condylar cartilage, tb-trabecular bone. Bar in A= 100μm. Quantification of TRAP staining (E). Each symbol on the graph represents measurements from one condyle. *Adamts5*$^{+/+}$ NL (open circle), *Adamts5*$^{+/+}$ 0.8N/10d (closed circle), *Adamts5*$^{-/-}$ NL (open squares), and *Adamts5*$^{-/-}$ 0.8N/10d (closed squares). Middle red bars represent the average of the mean with the

smaller upper and lower red bars indicating the standard deviation. *P=.017, ** P=.008; ***P=.001; Bar in A = 50 μm applies to B-D.